

Original Article

Involvement of nucleotide-binding oligomerization domain-like receptor family pyrin domain containing 3 inflammasome in the vascular dysfunction induced by high fat diet

Jiuhua Zhao^{1,2*}, Fengping Lin^{1*}, Zhenghong Zhang^{1*}, Qingqiang Lin^{1*}, Zhengchao Wang¹

¹Provincial Key Laboratory for Developmental Biology and Neurosciences, Provincial University Key Laboratory of Sport and Health Science, Key Laboratory of Optoelectronic Science and Technology for Medicine of Ministry of Education, College of Life Sciences, Fujian Normal University, Fuzhou 350007, China; ²West Anhui Health Vocational College, Luan 237005, China. *Equal contributors.

Received May 18, 2020; Accepted December 30, 2020; Epub April 15, 2021; Published April 30, 2021

Abstract: Objective: The past four decades have witnessed rapid improvement in living standards worldwide, and nutritional obesity has attracted increasing attention. To further understand the cardiovascular complications caused by a high-fat diet (HFD), there is an immediate need to focus on the effects of HFD on vascular structure and functions. Methods: The effects of HFD on physiological and biochemical indices were evaluated using ELISA kits, and the associated vascular abnormalities were investigated using microscopy and vasodilatation examination. Besides, NLRP3 inflammasome expression and activation were assessed by immunofluorescence, western blotting, and RT-qPCR assays. Results: Body weight and plasma insulin levels were found to be significantly increased in the HFD group by the third week, while fasting glucose concentrations and insulin resistance index apparently increased by the sixth week, and the changes in aortic structures occurred at the ninth week, suggesting that insulin resistance contributed to the elevated fasting glucose in the HFD group in a time-dependent pattern, following the pathological changes of aortic tissues. Further analysis showed increased expression and activation of NLRP3 inflammasome in the HFD group, which might have inhibited the vasodilatation during the sixth week. Conclusion: This study demonstrated the role of NLRP3 inflammasome in promoting HFD-induced vascular dysfunction.

Keywords: High-fat diet, NLRP3 inflammasome, vascular dysfunction

Introduction

With the improvement of living standards, the acceleration of work rhythm, the increase of learning pressure, and the change of eating habits, more and more people are now overweight or obese. Obesity is accompanied with some diseases, such as diabetes, hyperlipidemia, cardiovascular and cerebrovascular diseases, and fatty liver [1-3]. Therefore, obesity and associated diseases have become important concerns.

A high-fat diet (HFD) is widely used to induce obesity in animal models, which is the leading cause of type 2 diabetes. The global prevalence of obesity has increased rapidly, not only affect-

ing younger children but also seriously affecting human health, which led to the increased incidence of various endocrine diseases [3]. Previous studies have demonstrated that HFD induces vascular dysfunction, but the molecular mechanism remains to be elucidated. Some recent studies have suggested on the importance of the structure and function of NLRP3 inflammasome. The inflammasome is a polymer protein complex, which is composed of PRR, ASC, and caspase-1 [4-6], and implicated in functions in many pathophysiological processes, such as infection, identification, and tissue repair [7]. It has been found that some members of NLR and ALR families, including NLRP1, NLRP3, NLRC4, AIM2, and pyrin, can form inflammasomes [8-13]. NLRP3 inflamma-

some has been widely and deeply investigated and has been shown to possess NOD, LRR, and PYD domains for self-oligomerization, ligand recognition, and protein interaction, respectively [14-17]. ASC interacts with NLRP3 and caspase-1, and finally forms an NLRP3 inflammasome [18], which is essential for the immune defense [19], and can be activated by various exogenous [12, 20-22] and endogenous [23-25] stimulants.

At present, there are some reports about HFD-induced obesity, but the role of NLRP3 inflammasome in this process is still unclear. This study herein utilized HFD-induced obesity to elucidate the contribution of NLRP3 inflammasome to the changes of tissue structure and vascular function by examining NLRP3 expression, physiological and biochemical indices, vascular structure, and diastolic function, which will provide a clue for further studying its molecular mechanism.

Materials and methods

Animal ethics statement

The animal experiment was designed according to the Guide for the Care and Use of Laboratory Animals, and the protocol was also approved by the Fujian Normal University Authorization Committee (Approval Number: IACUC-2018-0015).

Animals and treatments

C57BL/6J mice (15.97±0.49 g body weight) were used in the present study. These mice were obtained from Wushi Experimental Animal Center (Fuzhou) and then raised in a standardized animal house with 23~25°C temperature, 50~60% humidity, and 12 h: 12 h light-dark cycle. They were randomly divided into two experimental groups after the preliminary experiment, one normal control diet (NCD) group and the other HFD group for 12 weeks, as described previously [26-28]. The fat contents in these two experimental diets were 12.0% and 66.5%, respectively (Table S1). Bodyweight monitoring was done to assess growth, and blood samples to determine glucose and insulin levels were collected weekly. Mice (n=6) from each group were anesthetized and sacrificed, following which the abdominal aorta was immediately isolated. Some seg-

ments of the aortic tissue were then fixed in 4% paraformaldehyde (PFA), and the remaining segments were frozen in liquid nitrogen for further examination, including vasodilative evaluation.

Determination of fasting plasma glucose and plasma insulin

Fasting glucose concentrations and plasma insulin levels were determined at the 0, 3rd, 6th, 9th and 12th week using the corresponding kit as described previously [26-28], and then the insulin resistance index was calculated. Briefly, fasting glucose concentrations were determined by a pin-prick technique after 12 h overnight starvation with the Accu-Chek test strip according to the manufacturer's protocol (Roche Diabetes Care, Burgess Hill, UK). Plasma insulin levels were determined using the Insulin Assay Kit (Nanjing Jiancheng Bioengineering Institute). The insulin resistance index (HOMA-IR) was calculated using the following formula.

$$\text{HOMA-IR} = (\text{fasting glucose} \times \text{plasma insulin}) / 22.5.$$

Histopathological evaluation of aortic tissues

The histopathological changes of the aortic tissues were evaluated as described previously [27-29]. Briefly, after the fixation of aortic segments, they were embedded into paraffin, then sectioned into 5 µm slides. These slides were dewaxed by 100% xylene, and then the tissues were hydrated by the gradient concentrations of ethyl alcohol, following with hematoxylin and eosin staining. After mounting, these slides were used for histopathological evaluation and examination of vessel wall thickness by a microscope.

Examination of vascular reactivity in vitro

The vascular reactivity of dissected arteries was examined using the microvascular tension measurement system with Ach (acetylcholine, 10^{-9} ~ 10^{-5} M) after pre-contraction with phenylephrine (PE, 10^{-9} M). Briefly, the isolated vessels were cut into two 3-4 mm wide rings, and the endothelium was carefully preserved. The vascular rings were suspended into an organ tank containing 10 mL Krebs solution and connected with the measurement system. One

NLRP3 inflammasome and vascular dysfunction

micromolar PE was used to constrict the vascular rings, and Ach was used to induce vasodilation, following which, the tension curve was recorded. Finally, the vascular reactivity was expressed as the percent relaxation of PE-induced pre-contraction.

Immunofluorescent staining for NLRP3 and ASC

Immunofluorescence was used to study the localization of NLRP3 and ASC. Briefly, the sections were incubated with a rabbit anti-NLRP3 antibody (1:500, Abcam) and a goat anti-ASC antibody (1:500, Abcam) at 4°C overnight. The immunofluorescent staining for NLRP3 and ASC was visualized using the FITC-labeled goat anti-rabbit IgG and Cy3-labeled donkey anti-goat IgG (Beyotime Institute of Biotechnology, Jiangsu, China) and then mounted with the cover-slips. Besides, the goat or rabbit serum (1:100; Boster Biological Technology, Wuhan) was used as a negative control. All of these slides were then photographed under a fluorescence microscope.

Western blotting for protein expression levels

The expression levels of NLRP3 inflammasome related proteins in aortic segments were detected by western blotting as described previously [14, 29-31]. Briefly, the tissues were homogenized in ice-cold RIPA buffer (Beyotime, Jiangsu) and extracted by centrifuging, followed by the estimation of protein concentrations using a BCA kit (Beyotime). After that, 20 µg of protein samples were loaded for separation by SDS-PAGE (Beyotime) and then transferred onto PVDF membrane (Beyotime). The PVDF membrane was then incubated with NLRP3 (1:1000, Abcam), ASC (1:1000, Abcam), pro-caspase-1 (1:1000, Abcam), cleaved-caspase-1 (1:1000, Abcam), IL-1β (1:500, Abcam) and β-actin (1:5000, Novus Biologicals) antibodies at 4°C overnight after blocking. After washing, membranes were incubated with HRP-labeled secondary antibodies (1:2,000, Beyotime), and bands were detected using the BeyoECL Star Western Blotting Detection reagent (Beyotime). β-actin expression was used as the loading control.

RT-qPCR analysis

Total RNA was extracted using TRIzol (Bio-Rad), reversed using cDNA Synthesis Kit (Bio-Rad),

and then amplified using TaqMan Gene Expression Assay kit (Applied Biosystems), including TaqMan Universal PCR Master Mix, NLRP3 primer (Hs00918082_m1), ASC primer (Hs00996676_m1) and 18S primer (Rn-03928990_g1). The levels of 18S ribosomal RNA were used as an endogenous control. Their expression levels were expressed as $2^{-\Delta\Delta Ct}$ values.

Assay of caspase-1 activity and IL-1β production

Caspase-1 activity and IL-1β were analyzed using a caspase-1 colorimetric assay kit (BioVision) and IL-1β enzyme-linked immunosorbent assay (ELISA) kit (Bender Medsystems), respectively, according to the manufacturer's protocol.

Statistical analysis

Data are presented as means ± SE. The significance ($P < 0.05$) between groups was evaluated by a one-way ANOVA (SPSS19.0), followed by a Tukey's multiple range test.

Results

Effects of HFD on body weight and fasting glucose

Initially, there was no obvious difference of the average body weight between the two groups. However, after 3 weeks, mice in the HFD group demonstrated time-dependent increases in body weight (**Figure 1A**). At 12 weeks, the average body weight of the HFD group (29.18 ± 1.38 g) was significantly heavier than that of the NCD group (21.06 ± 0.69 g). The levels of fasting plasma glucose were not significantly different between the two groups till the third week, but they were significantly higher in the HFD group than in the NCD group in the sixth week (**Figure 1B**). These results demonstrated that HFD increased the body weight and led to elevated levels of fasting glucose.

Effects of HFD on plasma insulin and insulin resistance

Considering the effects of insulin on fasting glucose, we also examined the changes in plasma insulin levels and observed a significant time-dependent increase in the HFD group (**Figure 2A**). In addition, the insulin resistance index

NLRP3 inflammasome and vascular dysfunction

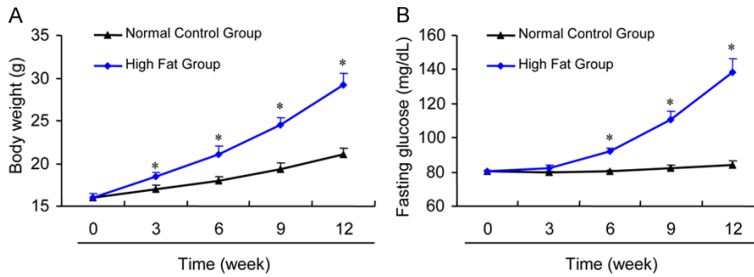


Figure 1. Effects of HFD on body weight (A) and fasting glucose (B).

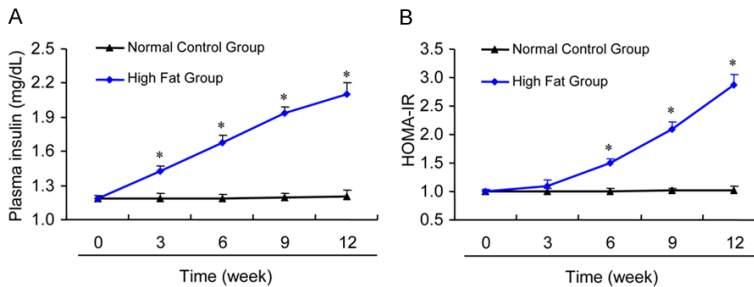


Figure 2. Effects of HFD on plasma insulin (A) and insulin resistance (B).

(HOMA-IR, **Figure 2B**) was not significantly different between the two groups till the third week (**Figure 2**), but increased significantly in the HFD group in the sixth week, corresponding with the change in plasma insulin concentrations (**Figure 2**). These results indicate that insulin regulated the fasting glucose levels for 3 weeks (**Figure 2**), but after 6 weeks, high insulin resistance led to elevated fasting glucose levels (**Figure 2**).

Effects of HFD on structural changes of aortic tissues

For further understanding of the pathological effect of HFD, histological structures of aortic tissues were examined, and no dramatic changes were observed till the 6th week (**Figure 3A-C, 3F, 3G, 3H**). However, apparent changes were observed from the 9th week (**Figure 3D, 3E, 3I, 3J**) in the HFD group (**Figure 3**). These morphological changes included serious endothelial damage, an incomplete endothelial layer, and an increased thickness of the aortic medial layer (**Figure 3I and 3J**), implying structural damage during the 9th week.

Effects of HFD on the thickness of aortic tissues

To confirm the morphological changes of histological structures, the thickness of aortic tis-

sues was measured, and no dramatic changes were observed in the aortic walls (**Figure 4B**) and medial layers (**Figure 4A**) till the 6th week. However, a considerable change in the aortic walls (**Figure 4B**) and medial layers (**Figure 4A**) was noted in the HFD group during the 9th week (**Figure 4**). These results demonstrated that structural changes occurred after physiological and biochemical indices, implying that the vascular function may also be changed before the tissue structure.

Effects of HFD on vascular endothelium-dependent function

Based on the above findings, the endothelium-dependent vasodilatation at the 6th week, with elevated fasting glucose and unchanged morphological structure was examined; the diastolic degree of the aorta in the NCD group increased gradually and dose-dependently (**Figure 5**), while the diastolic degree in the HFD group was significantly lower compared with the NCD group after treatment with acetylcholine (Ach) at gradient concentrations (**Figure 5**). These results indicated that endothelium-dependent vasodilatation was inhibited and damaged before the structural changes, implying that the molecular mechanism regulating the vascular functions may also be changed before the tissue structure.

Effects of HFD on expression and localization of NLRP3 inflammasome

Given that NLRP3 inflammasome is involved in many pathophysiological processes, this study detected the expression and localization of NLRP3 inflammasome using immunofluorescence in these two groups in the sixth week (**Figure 6**). The core proteins, NLRP3 and ASC, were mainly expressed in the vascular endothelial cells (**Figure 6**) and increased in the HFD group (**Figure 6C and 6D**) compared with the NCD group (**Figure 6A and 6B**). Their increased co-localization demonstrated that HFD activated NLRP3 inflammasome, followed by the inhibition of endothelium-dependent vasodilatation.

NLRP3 inflammasome and vascular dysfunction

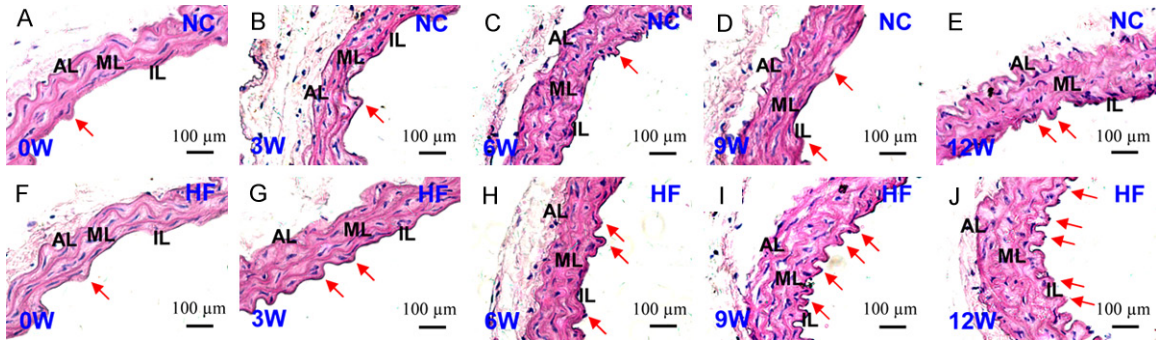


Figure 3. Effects of HFD on structural changes of aortic tissues. The adventitial (AL), medial (ML), intimal (IL), and endothelial (arrow) layers were observed in NCD (A-E) and HFD (F-J) groups. Scale bar = 100 μm .

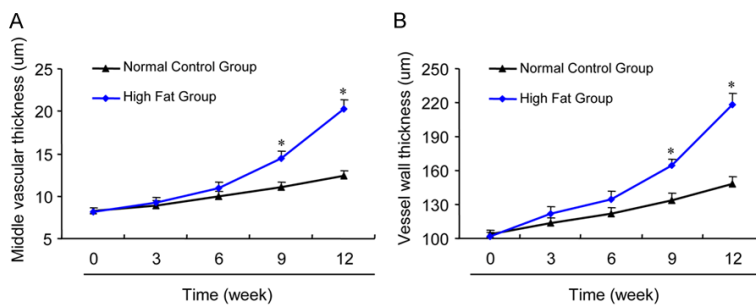


Figure 4. Effects of HFD on the thickness of aortic tissues. The thickness changes of the aortic medial layer (A) and aortic well (B) were compared between NCD and HFD groups. $n=6$. *: $P<0.05$, v.s. NCD.

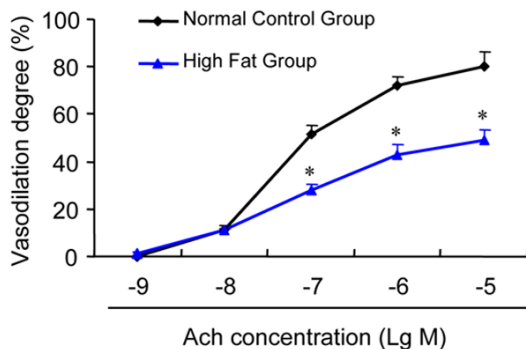


Figure 5. Effects of HFD on vascular endothelium-dependent functions. The endothelium-dependent vasodilatation was assessed using acetylcholine (Ach) in gradient concentrations at the 6th week. $n=6$. *: $P<0.05$, v.s. NCD.

Effects of HFD on NLRP3 inflammasome related proteins

Furthermore, this study examined the changes in expression levels of NLRP3, ASC, pro-caspase-1, cleaved-caspase-1, and IL-1 β proteins during NLRP3 inflammasome activation in the sixth week. NLRP3 and ASC were significantly

increased in the HFD group (Figure 7A and 7B), consistent with the above findings. Cleaved-caspase-1 and IL-1 β levels also increased considerably (Figure 7A and 7B), accompanied by decreased levels of pro-caspase-1 in the HFD group (Figure 7A and 7B), suggesting that NLRP3 inflammasome is activated before structural changes.

Effects of HFD on NLRP3 and ASC mRNA expression levels, caspase-1 activity and IL-1 β production

Finally, the mRNA expression levels of NLRP3 and ASC were determined; significantly increased mRNA expression levels of NLRP3 and ASC were observed in the HFD group (Figure 8A), which were consistent with the above results. Caspase-1 activity was found to be increased dramatically in the HFD group compared with the NCD group (Figure 8B), which was consistent with decreased pro-caspase-1 and increased cleaved-caspase-1. Additionally, IL-1 production in the HFD group was considerably higher than the NCD group (Figure 8C), which was similar to the above findings. All these results further demonstrated that NLRP3 inflammasome activation might contribute to this vascular dysfunction.

Discussion

In the present experiment, mice were fed with a HFD for a long term, and the biochemical indices, vascular structure, and diastolic function were assessed. The results demonstrated that HFD not only damaged the aortic structure but

NLRP3 inflammasome and vascular dysfunction

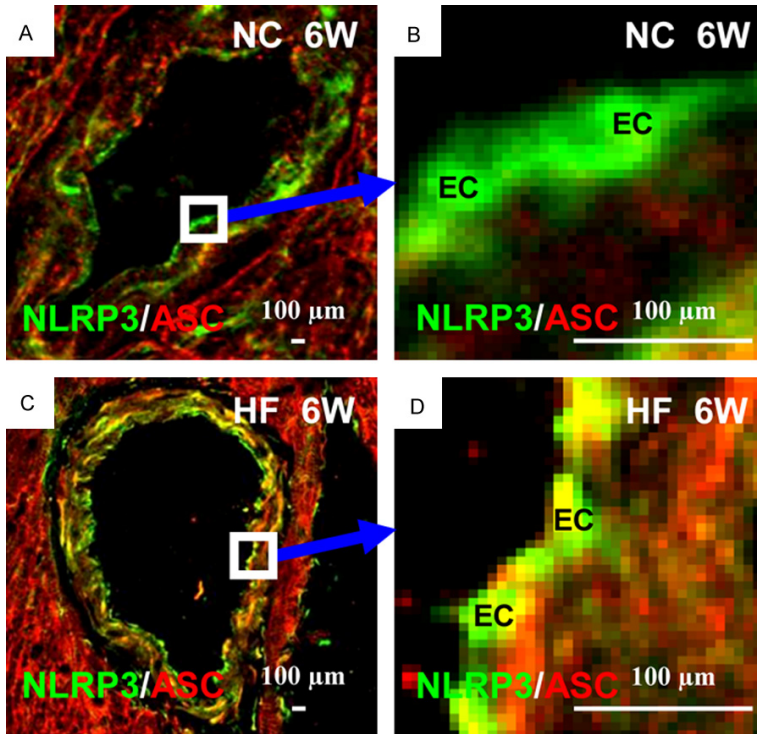


Figure 6. Effects of HFD on NLRP3 inflammasome expression. The expression levels of NLRP3 (green)/ASC (red) and their co-localization (yellow) were examined by immunofluorescence in NCD (A and B) and HFD (C and D) groups. Their co-localization (yellow) indicated NLRP3 inflammasome activation in endothelial cells (ECs). Scale bar = 100 μ m.

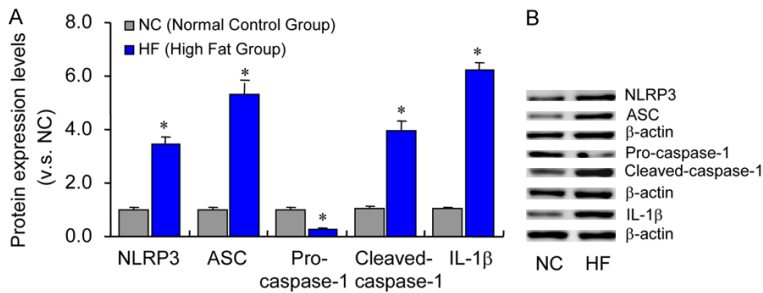


Figure 7. Effects of HFD on NLRP3 inflammasome related proteins. The expression levels of NLRP3, ASC, pro-caspase-1, cleaved-caspase-1, and IL-1 β were compared by summarized data (A) and blotting images (B) between NCD and HFD groups. n=6. *: $P < 0.05$, v.s. NCD.

also affected the diastolic function, which provided vital experimental data and reference for the prevention of obesity and related diseases.

During recent years, nutritional obesity caused by a high-fat diet has attracted more and more attention [32-46], which not only affected human health adversely but also resulted in a

significant increase in reproductive endocrine diseases [42-46]. The pathophysiological changes in obesity are mainly associated with an increase in the number and volume of fat cells and the infiltration of macrophages in fat tissues [3, 32, 33]. Hypertrophic and proliferative adipocytes can reduce the density, number, and activity of insulin receptors, and also activate some kinases to damage insulin signaling by increasing the serine phosphorylation level of IRS, thus promoting insulin resistance [42-46]. In turn, insulin resistance promotes obesity and forms a vicious circle [42-46]. This suggests that obesity is the main factor that causes insulin resistance. With the progress of the disease, the number and function of β cells in obese and insulin resistant individuals eventually decline, and the signaling pathway is also damaged [3, 47]. Here, HFD not only induced obesity but also resulted in type 2 diabetes mellitus since the levels of fasting glucose, plasma insulin, and insulin resistance in the HFD group were higher than those in the NCD group from the sixth week and increased in a time-dependent manner.

Clinical investigations have shown that the incidence of vascular complications is significantly higher in patients with hyperglycemia and diabetes mellitus than those with well-controlled blood glucose [3]. Long-term hyperglycemia is the root of diabetic vascular complications, and the clinical treatment of diabetes mellitus mainly involves controlling the blood glucose [48, 49]. Hypoglycemic drugs are often used to decrease the blood glucose level, and insulin sensitivity of peripheral tissues can be increased to reduce the blood

NLRP3 inflammasome and vascular dysfunction

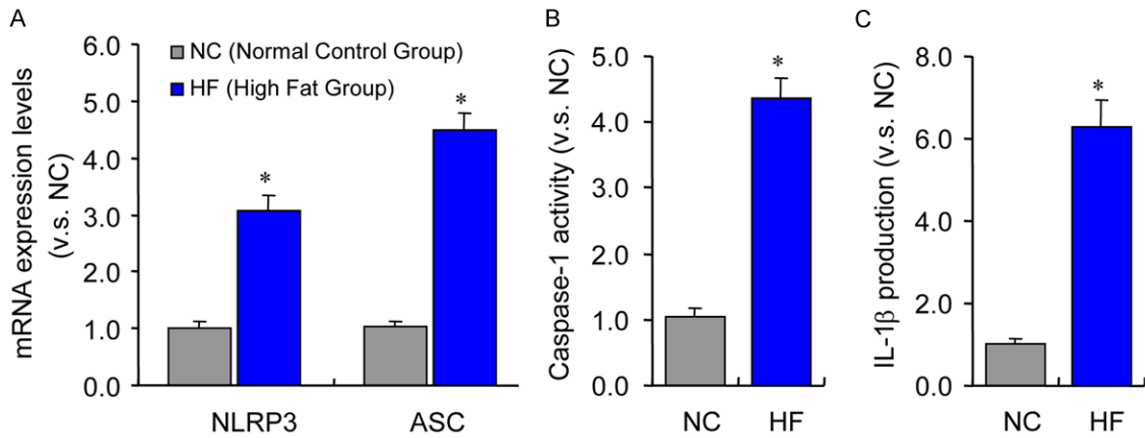


Figure 8. Effects of HFD on mRNA expression levels of NLRP3 and ASC (A), caspase-1 activity (B), and IL-1 β production (C) between NCD and HFD groups. n=6. *: $P < 0.05$, v.s. NCD.

glucose levels [50]. Diabetic vascular complications may be microvascular or macrovascular; microvascular complications mainly include retinopathy, neuropathy, and nephropathy, while macrovascular complications include cardiovascular and cerebrovascular diseases. Macrovascular complications are the leading cause of myocardial infarction and stroke, accounting for 80% of the deaths caused by type 2 diabetes mellitus [3, 51, 52]. Thus, it is particularly important to alleviate the macrovascular complications while treating diabetes mellitus. In the present study, no significant difference was observed in the vascular structure between the two groups before the 6th week. However, significant pathological changes were observed in the HFD group after the 9th week, which included damaged endothelial layer and thickened medial layer compared to the NCD group. Further investigation showed that diastolic degree of abdominal aorta in HFD group was obviously lower than NCD group at the 6th week, indicating that endothelium-dependent vasodilatation was affected in the HFD group prior to tissue structures.

Inflammation contributes to the pathogenesis of diabetes mellitus and vascular complications, and is a common feature of cardiovascular disease [51-53]. The blood vessels show endothelial damage and dysfunction during the early stage of diabetes mellitus [54, 55], and with the further development of this disease, lipid-protein enters the vascular wall through the damaged endothelial cells, promotes the platelet aggregation, activates the expression

of endothelial adhesion molecules, and accelerates the infiltration of inflammatory cells, finally leading to vascular inflammation [51-53]. Inflammation is crucial during the whole process of vascular diseases, and vascular inflammation is the main cause of diabetic vascular disease [3]. Long-term hyperglycemia stimulates vascular endothelial cells to transport a large amount of glucose to the endothelial cells, increases the glucose concentration in these cells, leads to the functional changes of mitochondria and proteins in endothelial cells, and lastly, results in vascular endothelial dysfunction [54, 55]. Hyperglycemia also stimulates vascular endothelial cells to produce excessive ROS and activates inflammation-related signaling pathway, inducing vascular inflammation [3]. NLRP3 inflammasome not only participates in innate immunity but also contributes to immune responses and disease occurrences, especially various inflammatory diseases [14-16, 31]. To elucidate the molecular mechanism of endothelium-dependent dysfunctions of the abdominal aorta in the 6th week, the localization and expression of NLRP3 inflammasome in the aortic tissues were examined. The results demonstrated that NLRP3 inflammasome was mainly expressed in the endothelial cells, and its levels in the HFD group were dramatically higher than the NCD group, indicating that HFD inhibited the endothelium-dependent vasodilatation through NLRP3 inflammasome activation in endothelial cells.

In conclusion, long-term HFD feeding not only caused obesity but also induced pathological

changes such as the elevation of fasting glucose and insulin resistance in the 6th week. Further, no apparent change in the tissue structure of the abdominal aorta between these two groups were observed in the 6th week, but endothelium-dependent vasodilation was affected in the HFD group, possibly via NLRP3 inflammasome activation in vascular endothelial cells; however, the detailed mechanism is still unclear. Therefore, the effects of HFD on vascular structure and functions and the underlying mechanisms might provide some important theoretical and experimental foundation for clinical prevention of obesity and related diseases.

Acknowledgements

This work was supported funded by National Training Program of Innovation and Entrepreneurship for Undergraduates (20191039-4023), Fujian Provincial Natural Science Foundation (2018J01721, 2018J01722 and 2020J01176), Fujian Province Science and Technology Project of The Education Department (JAT160118), Research Program of Excellent Young Talents in Colleges and Universities of Provincial Education Department (GXGNFX2019120), and the Educational Reform Project (Y201809 and P201801016) and Training Program of Innovation and Entrepreneurship for Undergraduates (CXXL-2020291 and CXXL2020293) of Fujian Normal University. We would like to thank the staff and Michael D. Wang in the Laboratory Animal Center, Fujian Normal University for their kind help during this project. We would also like to thank Editage (www.editage.com) for English language editing.

Disclosure of conflict of interest

None.

Abbreviations

HFD, high-fat diet; NCD, normal control diet; NLRP3, nucleotide-binding oligomerization domain-like receptor family pyrin domain containing 3; PRR, pattern recognition receptor; ASC, apoptosis associated speck like protein; NOD, nucleotide binding NACHT domain; LRR, leucine rich repeat; PYD, pyrimidine domain; NLR, NOD-like receptors; AIM2, the absent in melanoma 2; ALR, the absent in melanoma 2

(AIM2)-like receptor; HRP, horseradish peroxidase; IRS, insulin receptor substrate.

Address correspondence to: Dr. Zhengchao Wang, College of Life Sciences, Fujian Normal University, No. 8, Shangsang Road, Fuzhou 350007, China. Tel: +86-591-22868200; Fax: +86-591-22868200; E-mail: zchwang@fjnu.edu.cn

References

- [1] Mangan MSJ, Olhava EJ, Roush WR, Seidel HM, Glick GD and Latz E. Targeting the NLRP3 inflammasome in inflammatory diseases. *Nat Rev Drug Discov* 2018; 17: 588-606.
- [2] Zhou W, Chen C, Chen Z, Liu L, Jiang J, Wu Z, Zhao M and Chen Y. NLRP3: a novel mediator in cardiovascular disease. *J Immunol Res* 2018; 2018: 5702103.
- [3] Donath MY and Shoelson SE. Type 2 diabetes as an inflammatory disease. *Nat Rev Immunol* 2011; 11: 98-107.
- [4] Sutterwala FS, Haasken S and Cassel SL. Mechanism of NLRP3 inflammasome activation. *Ann N Y Acad Sci* 2014; 1319: 82-95.
- [5] Fan J, Xie K, Wang L, Zheng N and Yu X. Roles of inflammasomes in inflammatory kidney diseases. *Mediators Inflamm* 2019; 2019: 2923072.
- [6] Kanneganti TD, Lamkanfi M and Núñez G. Intracellular NOD-like receptors in host defense and disease. *Immunity* 2007; 27: 549-559.
- [7] Swanson KV, Deng M and Ting JP. The NLRP3 inflammasome: molecular activation and regulation to therapeutics. *Nat Rev Immunol* 2019; 19: 477-489.
- [8] Fernandes-Alnemri T, Yu JW, Datta P, Wu J and Alnemri ES. AIM2 activates the inflammasome and cell death in response to cytoplasmic DNA. *Nature* 2009; 458: 509-513.
- [9] Hornung V, Ablasser A, Charrel-Dennis M, Bauernfeind F, Horvath G, Caffrey DR, Latz E and Fitzgerald KA. AIM2 recognizes cytosolic dsDNA and forms a caspase-1-activating inflammasome with ASC. *Nature* 2009; 458: 514-518.
- [10] Xu H, Yang J, Gao W, Li L, Li P, Zhang L, Gong YN, Peng X, Xi JJ, Chen S, Wang F and Shao F. Innate immune sensing of bacterial modifications of Rho GTPases by the Pyrin inflammasome. *Nature* 2014; 513: 237-241.
- [11] Komada T and Muruvem DA. The role of inflammasomes in kidney disease. *Nat Rev Nephrol* 2019; 15: 501-520.
- [12] Martinon F, Burns K and Tschopp J. The inflammasome: a molecular platform triggering activation of inflammatory caspases and processing of proIL-beta. *Mol Cell* 2002; 10: 417-426.

NLRP3 inflammasome and vascular dysfunction

- [13] Broz P, Newton K, Lamkanfi M, Mariathasan S, Dixit VM and Monack DM. Redundant roles for inflammasome receptors NLRP3 and NLRC4 in host defense against Salmonella. *J Exp Med* 2010; 207: 1745-1755.
- [14] Zhang Z, Wang F and Zhang Y. Expression and contribution of NLRP3 inflammasome during the follicular development induced by PMSG. *Front Cell Dev Biol* 2019; 7: 256.
- [15] Shi C, Yang H and Zhang Z. Involvement of nucleotide-binding oligomerization domain-like receptor family pyrin domain containing 3 inflammasome in the pathogenesis of liver diseases. *Front Cell Dev Biol* 2020; 8: 139.
- [16] Zhang H and Wang Z. Effect and regulation of the NLRP3 inflammasome during renal fibrosis. *Front Cell Dev Biol* 2020; 7: 379.
- [17] Strowig T, Henao-Mejia J, Elinav E and Flavell R. Inflammasomes in health and disease. *Nature* 2012; 481: 278-286.
- [18] Medzhitov R. Origin and physiological roles of inflammation. *Nature* 2008; 454: 428-435.
- [19] Man SM and Kanneganti TD. Regulation of inflammasome activation. *Immunol Rev* 2015; 265: 6-21.
- [20] Dostert C, Pétrilli V, Van Bruggen R, Steele C, Mossman BT and Tschopp J. Innate immune activation through Nalp3 inflammasome sensing of asbestos and silica. *Science* 2008; 320: 674-677.
- [21] Allen IC, Scull MA, Moore CB, Holl EK, McElvania-TeKippe E, Taxman DJ, Guthrie EH, Pickles RJ and Ting JP. The NLRP3 inflammasome mediates in vivo innate immunity to influenza A virus through recognition of viral RNA. *Immunity* 2009; 30: 556-565.
- [22] Wu J, Fernandes-Alnemri T and Alnemri ES. Involvement of the AIM2, NLRC4, and NLRP3 inflammasomes in caspase-1 activation by *Listeria monocytogenes*. *J Clin Immunol* 2010; 30: 693-702.
- [23] Mariathasan S, Weiss DS, Newton K, McBride J, O'Rourke K, Roose-Girma M, Lee WP, Weinrauch Y, Monack DM and Dixit VM. Cryopyrin activates the inflammasome in response to toxins and ATP. *Nature* 2006; 440: 228-232.
- [24] Martinon F, Pétrilli V, Mayor A, Tardivel A and Tschopp J. Gout-associated uric acid crystals activate the NALP3 inflammasome. *Nature* 2006; 440: 237-241.
- [25] Zhou R, Tardivel A, Thorens B, Choi I and Tschopp J. Thioredoxin-interacting protein links oxidative stress to inflammasome activation. *Nat Immunol* 2010; 11: 136-140.
- [26] Rato L, Duarte AI, Tomás GD, Santos MS, Moreira PI, Socorro S, Cavaco JE, Alves MG and Oliveira PF. Pre-diabetes alters testicular PGC1- α /SIRT3 axis modulating mitochondrial bioenergetics and oxidative stress. *Biochim Biophys Acta* 2014; 1837: 335-344.
- [27] Wang S, Li J, Zhang C, Xu G, Tang Z, Zhang Z, Liu Y and Wang Z. Effects of aerobic exercise on the expressions and activities of nitric oxide synthases in the blood vessel endothelium in prediabetes mellitus. *Exp Ther Med* 2019; 17: 4205-4212.
- [28] Wu Y, Zhang Z, Liao X, Qi L, Liu Y and Wang Z. Effect of high-fat diet-induced obesity on the Akt/FoxO/Smad signaling pathway and the follicular development of the mouse ovary. *Mol Med Rep* 2016; 14: 3894-3900.
- [29] Wu Y, Li Y, Liao X, Wang Z, Li R, Zou S, Jiang T, Zheng B, Duan P and Xiao J. Diabetes induces abnormal ovarian function via triggering apoptosis of granulosa cells and suppressing ovarian angiogenesis. *Int J Biol Sci* 2017; 13: 1297-1308.
- [30] Zhang Z, Yin D and Wang Z. Contribution of hypoxia-inducible factor-1 α to transcriptional regulation of vascular endothelial growth factor in bovine developing luteal cells. *Anim Sci J* 2011; 82: 244-50.
- [31] Wang F, Wang S, Zhang Z, Lin Q, Liu Y, Xiao Y, Xiao K and Wang Z. Activation of NLRP3 inflammasome in the ovaries during the development and treatment of polycystic ovary syndrome. *Int J Clin Exp Pathol* 2017; 10: 5022-5030.
- [32] Zheng J, Manabe Y and Sugawara T. Siphonaxanthin, a carotenoid from green algae *Codium cylindricum*, protects Ob/Ob mice fed on a high-fat diet against lipotoxicity by ameliorating somatic stresses and restoring anti-oxidative capacity. *Nutr Res* 2020; 77: 29-42.
- [33] Wang P, Li D, Ke W, Liang D, Hu X and Chen F. Resveratrol-induced gut microbiota reduces obesity in high-fat diet-fed mice. *Int J Obes (Lond)* 2020; 44: 213-225.
- [34] Hassan AM, Mancano G, Kashofer K, Fröhlich EE, Matak A, Mayerhofer R, Reichmann F, Olivares M, Neyrinck AM, Delzenne NM, Claus SP and Holzer P. High-fat diet induces depression-like behaviour in mice associated with changes in microbiome, neuropeptide Y, and brain metabolome. *Nutr Neurosci* 2019; 22: 877-893.
- [35] Zhao M, Jiang Z, Cai H, Li Y, Mo Q, Deng L, Zhong H, Liu T, Zhang H, Kang JX and Feng F. Modulation of the gut microbiota during high-dose glycerol monolaurate-mediated amelioration of obesity in mice fed a high-fat diet. *mBio* 2020; 11: e00190-20.
- [36] Son HK, Shin HW, Jang ES, Moon BS, Lee CH and Lee JJ. Gochujang prepared using rice and wheat koji partially alleviates high-fat diet-induced obesity in rats. *Food Sci Nutr* 2020; 8: 1562-1574.
- [37] Zhang J, Zhao Y, Ren D and Yang X. Effect of okra fruit powder supplementation on metabolic syndrome and gut microbiota diversity in

NLRP3 inflammasome and vascular dysfunction

- high fat diet-induced obese mice. *Food Res Int* 2020; 130: 108929.
- [38] Micioni Di Bonaventura MV, Martinelli I, Moruzzi M, Micioni Di Bonaventura E, Giusepponi ME, Polidori C, Lupidi G, Tayebati SK, Amenta F, Cifani C and Tomassoni D. Brain alterations in high fat diet induced obesity: effects of tart cherry seeds and juice. *Nutrients* 2020; 12: 623.
- [39] Xu J, Ma Z, Li X, Liu L and Hu X. A more pronounced effect of type III resistant starch vs. type II resistant starch on ameliorating hyperlipidemia in high fat diet-fed mice is associated with its supramolecular structural characteristics. *Food Funct* 2020; 11: 1982-1995.
- [40] Terzo S, Mulè F, Caldara GF, Baldassano S, Puleio R, Vitale M, Cassata G, Ferrantelli V and Amato A. Pistachio consumption alleviates inflammation and improves gut microbiota composition in mice fed a high-fat diet. *Int J Mol Sci* 2020; 21: 365.
- [41] Han Y, Park H, Choi BR, Ji Y, Kwon EY and Choi MS. Alteration of microbiome profile by D-allulose in amelioration of high-fat-diet-induced obesity in mice. *Nutrients* 2020; 12: 352.
- [42] Uchikawa M, Kato M, Nagata A, Sanada S, Yoshikawa Y, Tsunematsu Y, Sato M, Suzuki T, Hashidume T, Watanabe K, Yoshikawa Y and Miyoshi N. Elevated levels of proinflammatory volatile metabolites in feces of high fat diet fed KK-Ay mice. *Sci Rep* 2020; 10: 5681.
- [43] Kwon EY and Choi MS. Eriocitrin improves adiposity and related metabolic disorders in high-fat diet-induced obese mice. *J Med Food* 2020; 23: 233-241.
- [44] Cloutier F, Roumaud P, Ayoub-Charette S, Chowdhury S and Martin LJ. The intake of an extract from seeds of *Tamarindus indica* L. modulates the endocrine function of adult male mice under a high fat diet. *Heliyon* 2020; 6: e03310.
- [45] Li T, Gong H, Yuan Q, Du M, Ren F and Mao X. Supplementation of polar lipids-enriched milk fat globule membrane in high-fat diet-fed rats during pregnancy and lactation promotes brown/beige adipocyte development and prevents obesity in male offspring. *FASEB J* 2020; 3: 4619-4634.
- [46] Héliers-Toussaint C, Fouché E, Naud N, Blas-Y-Estrada F, Del Socorro Santos-Diaz M, Nègre-Salvayre A, Barba de la Rosa AP and Guéraud F. *Opuntia cladode* powders inhibit adipogenesis in 3 T3-F442A adipocytes and a high-fat-diet rat model by modifying metabolic parameters and favouring faecal fat excretion. *BMC Complement Med Ther* 2020; 20: 33.
- [47] Wang F, Wang S, Zhang Z, Lin Q, Liu Y, Xiao Y, Xiao K and Wang Z. Defective insulin signaling and the protective effects of dimethyldiguanide during follicular development in the ovaries of polycystic ovary syndrome. *Mol Med Rep* 2017; 16: 8164-8170.
- [48] Gorshtein A, Shimon I, Shochat T, Amitai O and Akirov A. Long-term outcomes in older patients with hyperglycemia on admission for ischemic stroke. *Eur J Intern Med* 2018; 47: 49-54.
- [49] Xiong C, Wu Q, Fang M, Li H, Chen B and Chi T. Protective effects of luteolin on nephrotoxicity induced by long-term hyperglycaemia in rats. *J Int Med Res* 2020; 48: 300060520903642.
- [50] Hulst AH, Preckel B, Hollmann MW, DeVries JH and Hermanides J. Preoperative continuation of oral hypoglycemic drugs. *Anesth Analg* 2019; 128: e49.
- [51] Artasensi A, Pedretti A, Vistoli G and Fumagalli L. Type 2 diabetes mellitus: a review of multi-target drugs. *Molecules* 2020; 25: 1987.
- [52] Thakarakkattil Narayanan Nair A, Donnelly LA, Dawed AY, Gan S, Anjana RM, Viswanathan M, Palmer CNA and Pearson ER. The impact of phenotype, ethnicity and genotype on progression of type 2 diabetes mellitus. *Endocrinol Diabetes Metab* 2020; 3: e00108.
- [53] Si Y, Wang C, Guo Y, Yin H and Ma Y. Prevalence of osteoporosis in patients with type 2 diabetes mellitus in the Chinese mainland: a protocol of systematic review and meta-analysis. *Medicine (Baltimore)* 2020; 99: e19762.
- [54] Liu Y, Li J, Zhang Z, Tang Y, Chen Z and Wang Z. Endocrinological analysis of endothelium-dependent vasodilation in middle-aged patients with impaired glucose tolerance during prediabetes mellitus. *Exp Ther Med* 2014; 7: 697-702.
- [55] Liu Y, Li J, Zhang Z, Tang Y, Chen Z and Wang Z. Effects of exercise intervention on vascular endothelium functions of patients with impaired glucose tolerance during prediabetes mellitus. *Exp Ther Med* 2013; 5: 1559-1565.

NLRP3 inflammasome and vascular dysfunction

Table S1. Composition of experimental diets fed to the animals

	Normal Control Diet	High Fat Diet
Methionine (g/kg)	3.0	3.5
Vitamin mix (g/kg)	10.0	11.7
Mineral mix (g/kg)	35.0	41.0
Choline chloride (g/kg)	2.0	2.3
Cellulose (g/kg)	50.0	58.5
Casein (g/kg)	224.0	324.0
Corn starch (g/kg)	625.0	155.0
Corn oil (g/kg)	51.0	74.0
Lard (g/kg)	0	333.0
Protein (%)	21.5	21.5
Carbohydrate (%)	66.5	12.0
Fat (%)	12.0	66.5
Caroric density (kcal/g)	4.20	6.10

Note: The high fat diet contained 3.02 mg NaCl and 6.09 mg elemental calcium per gram, while the normal control diet contained 2.58 mg NaCl and 5.20 mg elemental calcium per gram, because of the differences in caloric density and anticipated food intake.